

1 **Large scale sequence-based screen for recessive variants**
2 **allows for identification and monitoring of rare deleterious**
3 **variants in pigs**

4 Anne Boshove^{1*}, Martijn F.L Derk^{1,2}, Claudia A. Sevillano¹, Marcos S. Lopes^{1,3}, Maren van Son⁴, Egbert F. Knol¹,
5 Bert Dibbits², Barbara Harlizius¹

6 ¹Topigs Norsvin Research Center, Beuningen, the Netherlands

7 ²Animal Breeding and Genomics, Wageningen University & Research, Wageningen, the Netherlands

8 ³Topigs Norsvin, Curitiba, Brazil

9 ⁴Norsvin SA, Hamar, Norway.

10

11 *Corresponding author

12 E-mail: anne.boshove@topigsnorsvin.com (AB)

13

14

15

16

17

18

19

20

21

22

23 Abstract

24 Most deleterious variants are recessive and segregate at relatively low frequency. Therefore, high sample sizes
25 are required to identify these variants. In this study we report a large-scale sequence based genome-wide
26 association study (GWAS) in pigs, with a total of 120,000 Large White and 80,000 Synthetic breed animals
27 imputed to sequence using a reference population of approximately 1,100 whole genome sequenced pigs. We
28 imputed over 20 million variants with high accuracies ($R^2 > 0.9$) even for low frequency variants (1-5% minor
29 allele frequency). This sequence-based analysis revealed a total of 13 additive and 8 non-additive significant
30 quantitative trait loci (QTLs) for growth rate and backfat thickness. With the non-additive (recessive) model,
31 we identified a deleterious missense SNP in the *CDHR2* gene reducing growth rate and backfat in homozygous
32 Large White animals. For the Synthetic breed, we revealed a QTL on chromosome 15 with a frameshift variant
33 in the *OBSL1* gene. This QTL has a major impact on both growth rate and backfat, resembling human 3M-
34 syndrome 2 which is related to the same gene. With the additive model, we confirmed known QTLs on
35 chromosomes 1 and 5 for both breeds, including variants in the *MC4R* and *CCND2* genes. On chromosome 1,
36 we disentangled a complex QTL region with multiple variants affecting both traits, harboring 4 independent
37 QTLs in the span of 5 Mb. Together we present a large scale sequence-based association study that provides a
38 key resource to scan for novel variants at high resolution for breeding and to further reduce the frequency of
39 deleterious alleles at an early stage in the breeding program.

40

41

42

43

44

45

46

47 Author Summary

48 In this study we investigated the effect of over 20 million genetic variants on the growth rate and backfat
49 thickness of approximately 140,000 pigs across two commercial breeds, with specific focus on recessive harmful
50 variation. We identified 14 regions with a significant additive effect and 8 regions with a significant recessive
51 effect on these traits. By looking at recessive effects we identified several rare deleterious variants with high
52 impacts on animal fitness. These include a deletion on chromosome 15 in the *OBSL1* gene, which leads to a
53 growth reduction of 100 grams a day on average. Interestingly, loss-of-function mutations in *OBSL1* are
54 associated with short stature in humans. Looking at additive effects with this high-resolution dataset allowed us
55 to gain more insight into the locus around the *MC4R* gene on chromosome 1. Here we found a small complex
56 region containing several independent variants affecting both growth rate and backfat. With this study we have
57 shown that by using several gene models and a large dataset, we can identify novel genetic variants at high
58 resolution (<0.01 frequency) with significant impact on animal fitness and production. These results can help us
59 in further eradicating deleterious genetic variants from pig populations.

60
61
62
63
64
65
66
67
68
69
70
71
72
73

74 Introduction

75 In livestock, genomic selection has accelerated genetic gain due to its major impact on increasing the accuracy
76 of breeding value estimation at a young age and reducing the generation interval [1]. Genomic selection, while
77 boosting desirable trait improvement, can inadvertently exacerbate the frequency of deleterious alleles. By
78 favoring individuals with superior trait-associated genetic markers, carriers of rare recessive deleterious alleles
79 can be unknowingly propagated in breeding populations, potentially leading to the expression of harmful
80 phenotypes in subsequent generations and compromising overall genetic health [2]. Balancing accelerated
81 genetic gain with the need to mitigate the accumulation of deleterious alleles becomes a critical consideration
82 in sustainable breeding strategies.

83 Deleterious recessive alleles can remain hidden because the harmful effects are only present in a homozygous
84 state, and their impact may not be fully captured by traditional additive genetic models [2]. Especially for low
85 frequency alleles, a large study population is crucial for identifying deleterious recessive alleles because the
86 number of homozygous animals for the minor allele is small. In addition, imputing to sequence is essential for
87 identifying deleterious alleles as it extends the scope of genetic analysis beyond genotyped variants, enabling
88 the discovery of rare and non-genotyped variants associated with deleterious effects [3]. Imputation is a method
89 that allows for predicting the genotypes of organisms at a higher density, based on a reference population of
90 which this higher density data is already available [4]. In commercial pig populations, imputation with good
91 accuracies is possible because there is a limited set of haplotypes segregating [5]. By performing imputation, we
92 accurately predict the large majority of genetic variation within populations as long as a sufficiently large
93 reference population is available. With whole genome sequencing (WGS) becoming more accessible and
94 affordable, it is now possible to obtain reference populations allowing for performing imputation up to whole
95 genome sequence level with high accuracies. Imputation to sequence is not only useful to fine map QTL regions,
96 but also to identify novel deleterious alleles affecting the fitness of animals by focusing on non-additive effects.
97 This can be done by performing genome-wide association studies (GWAS) using different models [6]. Previous
98 studies have identified non-additive (recessive) effects, mainly by focusing on depletion of homozygotes [7] [8].
99 This method allows for identifying recessive variants with lethal effects, but not recessive variants decreasing
100 fitness without leading to death.

101 By performing GWAS, we can test the association between SNPs and phenotypic records of traits of interest,
102 which allows us to identify quantitative trait loci (QTLs). Several models can be used for GWAS, with the additive
103 model being most commonly used [9]. An additive GWAS model assumes that the effects of different alleles on
104 the trait are cumulative and can be estimated linearly based on the number of alleles present. However, this
105 model can fail to pick up non-additive genetic variation, such as recessive and dominance effects. Recessive
106 effects are especially of interest when trying to identify deleterious variants [2]. To identify SNPs with recessive
107 effects, we can use a non-additive model. Recently several novel deleterious (coding) variants were identified in
108 cattle using a non-additive GWAS on imputed sequence of >100,000 individuals [10].

109 In this study, we performed imputation to sequence of 120,000 pigs of a Large White sow breed and 80,000 pigs
110 of a Synthetic boar breed. We performed GWAS on this imputed sequence data using both an additive and a
111 non-additive (recessive) model for the production traits growth rate (GR) and backfat (BF). Using the non-
112 additive model, we identified novel low frequent deleterious alleles affecting our traits of interest including loss-
113 of-function mutations that can be purged from the population.

114
115
116
117
118
119
120
121
122
123
124
125
126
127

128 Results

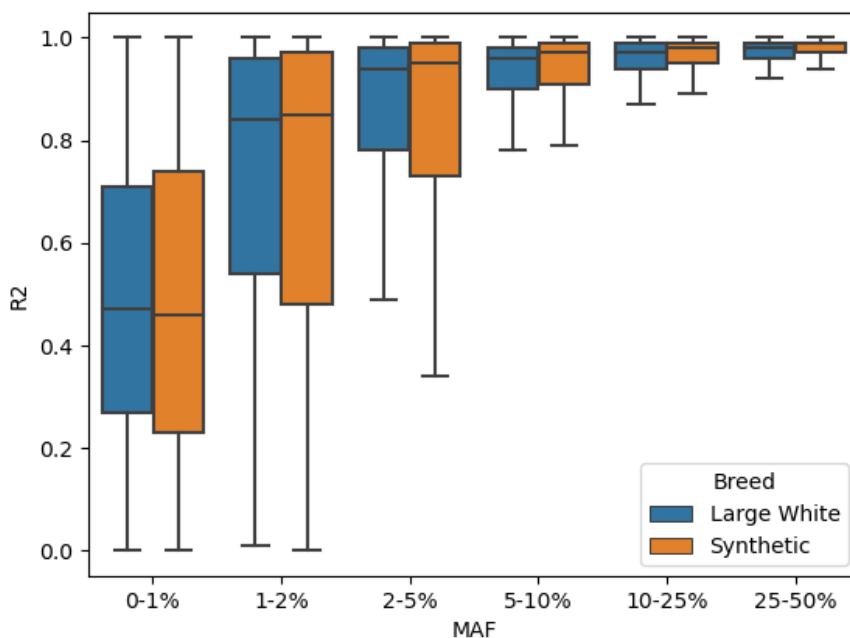
129 Imputation to sequence

130 The dataset consists of 120,147 Large White and 81,250 Synthetic animals genotyped on medium density SNP
131 panels (25K/50K). These animals were first imputed to 660K density with a reference population of 3500 animals.
132 Subsequently, the imputed 660K genotypes were imputed to whole genome sequence level, with a reference
133 population of 1069 animals (**S1 Figure**). We filtered the results to only include variants with an allele count of at
134 least 100. This gave us a total of 28,190,307 variants for Large White and 24,124,813 variants for Synthetic. The
135 majority of these variants were SNPs (**Table 1**). For SNPs with MAFs above 1-2% we were able to obtain very
136 good imputation accuracies ($R^2 > 0.9$), and even for half of the SNPs below 1% frequency we obtained accuracies
137 of $R^2 > 0.5$ (**Fig 1**).

138 **Table 1: Number of variants imputed to sequence split by variant type and MAF.**

	Large White		Synthetic	
	SNPs	Indels	SNPs	Indels
Total	22,840,678	5,349,629	19,398,280	4,726,533
< 1% MAF	4,329,777	600,075	4,496,085	641,335
< 5% MAF	8,109,989	1,472,040	7,510,302	1,400,929

139 MAF, minor allele frequency; SNP, single nucleotide polymorphism; Indel, insertion / deletion.

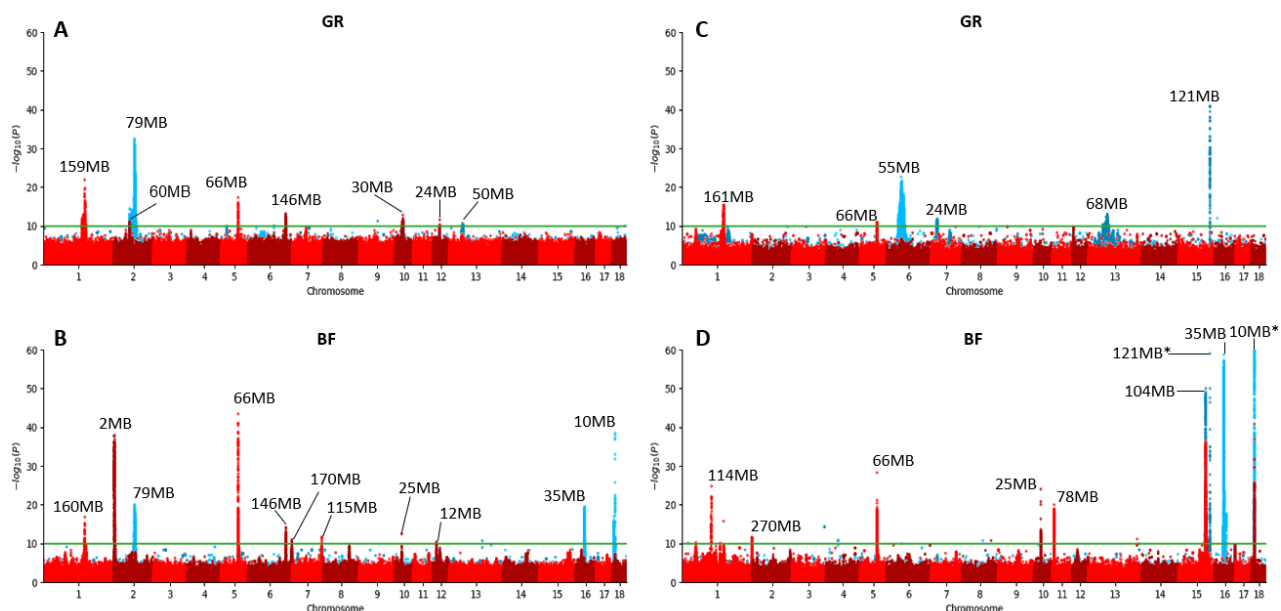


140

141 **Fig 1: Imputation accuracies (R2) of all SNPs grouped by Minor Allele Frequency (MAF)**

142 Additive and non-additive sequence-based GWAS on growth rate and backfat

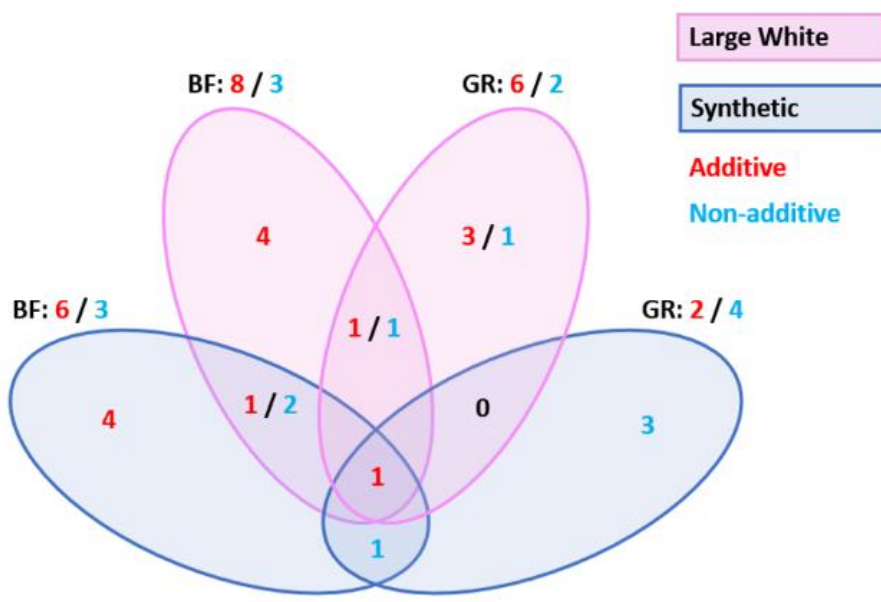
143 We performed both an additive and non-additive (recessive) GWAS on growth rate and backfat thickness in the
144 Large White (**Fig 2 A-B**) and Synthetic breed (**Fig 2 C-D**) using the imputed sequence data. For Large White, we
145 used 67K phenotypes for growth rate and 72K for backfat. For the Synthetic breed, we used 74K phenotypes for
146 both traits. From the results, we observe a large number of QTLs with distinct QTLs for additive and non-additive
147 effects. Across traits and breeds, we find a total of 14 additive and 8 non-additive QTLs, using a significance
148 threshold of p -value $< 1E-10$ (**Fig 3**). For each QTL, we examined the top SNPs and their associated effects on
149 genes using Ensembl VEP [11], SIFT scores [12] and pCADD scores [13], and we assessed the impact these QTLs
150 have on the phenotypes (**Fig 4, S2 Table**). We managed to identify potential causal variants for some of these
151 effects.



152 **Fig 2: Additive (red) and recessive (blue) Manhattan plots for growth rate (GR) and backfat (BF).** For peaks with a p -value
153 significance below $1E-10$ (green line) the genomic location is shown. QTLs only supported by a single significant SNP are
154 neglected. A) Large White growth rate B) Large White backfat C) Synthetic growth rate D) Synthetic backfat. *The 121MB
155 and 10MB peaks have top SNPs with p -values of $6,91E-154$ and $1,63E-135$ respectively.

156

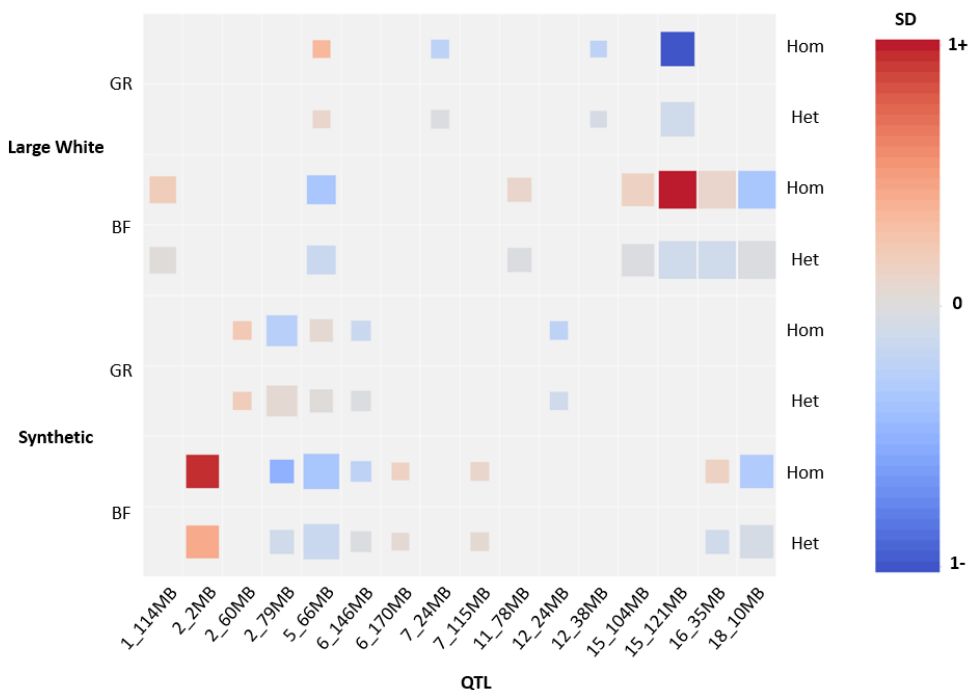
157



158

159 Fig 3: Number of significant GWAS QTLs overlapping between breeds and traits.

160



161 Fig 4: Phenotypic effect sizes of top SNPs from the significant QTLs

162 QTLs with phenotypic effects < 0.1 standard deviations are excluded. Square size indicates significance (bigger square is

163 lower *p*-value, ranging from 1E-10 to 1E-50+).

164 Non-additive GWAS identifies loss-of-function variants associated with poor
165 performance in homozygous individuals

166 **Non-additive effect on chromosome 2 shows decrease in growth rate and backfat in Large**
167 **White**

168 We find a very significant non-additive QTL on chromosome 2 for both growth rate and backfat. The QTL is
169 located around 79Mb with MAFs of 10%. The SNPs in this QTL show a negative impact on growth and backfat in
170 homozygous individuals, and a negligible effect in heterozygous individuals. Homozygous animals grow on
171 average 20 grams a day less (0.24 SDs) and have 0.7mm less backfat (0.47 SDs). The top SNP for growth is located
172 at 79,261,674bp and the top SNP for backfat is located at 79,236,726bp. Both SNPs are also present very
173 significantly in the other traits' GWAS. The QTLs consist mostly of intron variants of *ADAMTS2* (A Disintegrin-Like
174 and Metalloproteinase with Thrombospondin Type 1 Motif 2). Interestingly, the QTL comprises a deleterious
175 missense SNP (pCADD: 22.6, SIFT: 0) in the *CDHR2* (Cadherin-Related Family Member 2) gene at 81,336,954bp,
176 known to affect body size in knockout mice [14].

177 **Stop gain SNP in *ANKRD55* affects backfat levels in both Large White and Synthetic breeds**

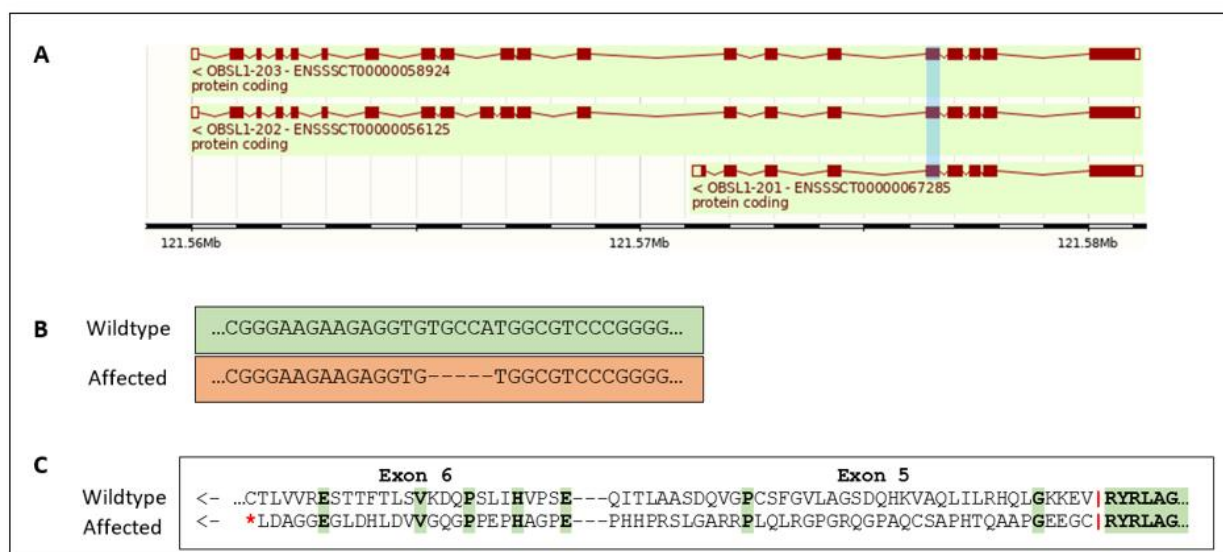
178 For backfat we find a very significant non-additive QTL on chromosome 16 that segregates in both breeds. The
179 SNPs in the QTL have a MAF of around 10% in Large White and 19% in the Synthetic breed. The top SNP for the
180 Synthetic breed and also a very significant SNP in the Large White GWAS is a stop gain SNP in the *ANKRD55*
181 (ankyrin repeat domain 55) gene, located at 35,245,909bp. Homozygous animals show increased backfat levels,
182 whereas heterozygous animals show some decrease in backfat. Homozygous animals have 0.29mm (0.17 SDs)
183 more backfat in the Large White breed and 0.18mm (0.13 SDs) more backfat in the Synthetic breed.
184 Heterozygous animals show 0.11mm less backfat in both breeds.

185 **Missense SNP in *MPIG6B* decreases growth rate in the Synthetic breed**

186 In the Synthetic breed, we observe a non-additive QTL on chromosome 7. Homozygous animals show a decrease
187 in growth of 30 grams a day (0.2 SDs). The fourth most significant SNP in this QTL is a deleterious missense SNP
188 (pCADD: 24.4, SIFT: 0.01) in *MPIG6B* (Megakaryocyte And Platelet Inhibitory Receptor G6b). The SNP is located
189 at 23,835,601bp with a MAF of 28%.

190 **Frameshift variant in *OBSL1* strongly affects growth rate and backfat the Synthetic breed**

191 In the Synthetic breed, we identified a very significant QTL for both growth rate and backfat on chromosome 15.
192 The top SNP is the same for both traits (121,500,039bp) and has a MAF of 5%. Homozygous animals show very
193 poor growth and highly elevated levels of backfat, growing on average around 100 grams a day less (-1.08 SDs)
194 and showing an increase in backfat of 2.2mm (2.24 SDs) compared to non-homozygotes. We identified the most
195 likely causal mutation to be a frameshift variant located at 121,576,506bp, in high LD with the top SNP from the
196 GWAS ($R^2=0.95$). The frameshift is caused by a 5bp deletion in the 5th exon of the *OBSL1* (Obscurin Like
197 Cytoskeletal Adaptor 1) gene (Fig 5 [15]). This induces a premature stop-codon in the 6th exon. To validate the
198 presence of the 5bp deletion we genotyped 31 pigs from three litters where the sow was carrier of the deletion
199 (using a dye-labeled primer). We confirmed the presence of the deletion and confirmed 15 carriers using this
200 test (Table S3).



201

202 **Fig 5: Genomic overview of the *OBSL1* frameshift variant**

203 A) *OBSL1* gene model adapted from Ensembl 110, exon 5 affected by the frameshift highlighted in blue. B) DNA sequence
204 alignment showing the 5bp deletion causing a frameshift in affected animals. C) Protein alignment showing the frameshift
205 inducing a premature stop-codon on exon 6.

206

207 Additive GWAS identifies known, novel, and complex QTLs with varying effects
208 on performance

209 **Additive model shows expected QTLs on chromosomes 1 and 5 in Large White and Synthetic
210 breed**

211 In the additive GWAS results we find two QTLs that we consistently observe when performing GWAS on these
212 traits. One is located on chromosome 1 where we find a missense SNP in the *MC4R* (melanocortin 4 receptor)
213 gene located at 160,773,437bp. This missense SNP has been described before, animals with the major allele (G)
214 show less backfat while animals with the minor allele (A) show faster growth [16], hence the QTL showing up for
215 both traits. On chromosome 5, we find a QTL especially significant for backfat. The top SNP of this QTL is an
216 intron variant of the *CCND2* (cyclin D2) gene affecting gene expression, located at 66,103,958bp. The G allele for
217 this SNP has been reported earlier to increase backfat [16].

218 **Low frequent additive QTL on chromosome 2 strongly affects backfat in Large White**

219 At the start of chromosome 2, we find a very significant novel QTL for backfat with SNPs located from 17Kb to
220 2.3Mb. These SNPs are very low frequent with MAFs between 0.4%-0.5%. Despite the low frequency, the SNPs
221 in the QTL have high imputation accuracies ($R^2 > 0.9$). Heterozygous animals on average have an increased backfat
222 thickness of around 0.7mm (0.43 SDs). Due to the very low frequency of these variants, our dataset only includes
223 3 homozygous animals, of which 2 show an increase in backfat of over 2.3mm (1.36 SDs). The QTL is located in
224 a region encompassing different genes including *NADSYN1* (NAD synthetase 1) , *INS* (Insulin) and *IGF2* (Insulin
225 like growth factor II). Both *INS* and *IGF2* play a role in glucose regulation and affect lipid metabolism, making
226 them interesting candidate genes for the phenotypic effects we observe in this QTL. Another significant SNP
227 present in the QTL is a missense SNP in *ANO9*, (anoctamin 9) located at 245,676bp with a pCADD score of 21.78.

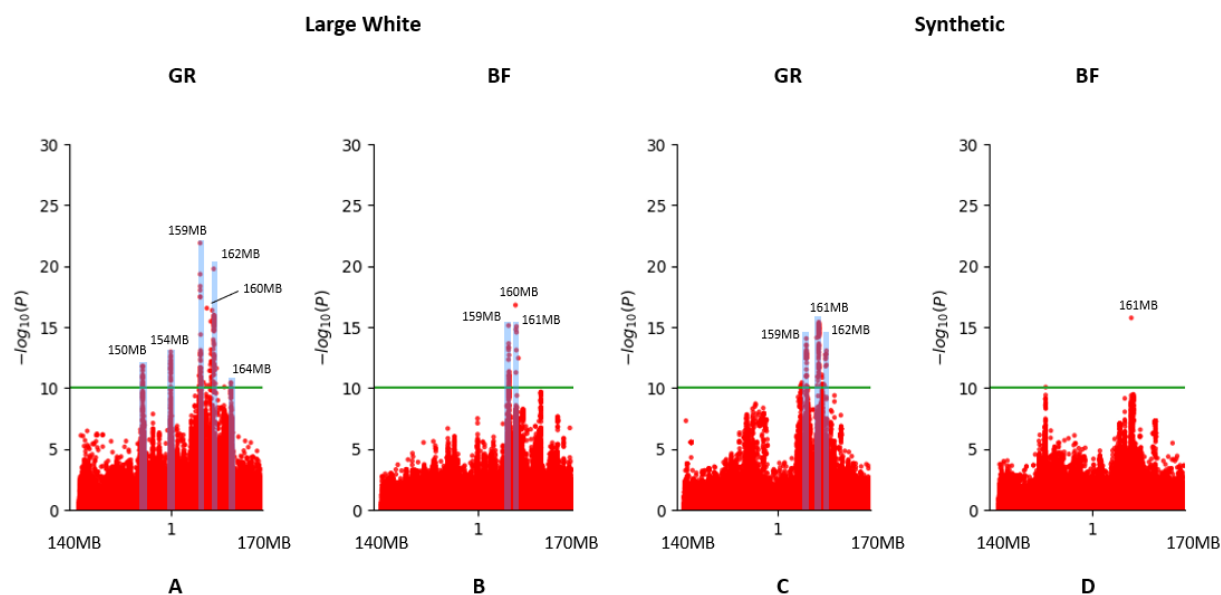
228

229

230

231 **Small complex region on chromosome 1 contains several independent variants affecting**
232 **growth rate and backfat**

233 On chromosome 1 we find a very complex region located from approximately 150-165Mb (Fig 6). This region is
234 present for both traits and both breeds, but most effects and highest significances are observed for growth rate
235 in Large White. In the Synthetic breed we find only a single significant SNP for backfat (Fig 6 D), which is also
236 present in the other breed and trait.



237

238 **Fig 6: Manhattan plots of region on chromosome 1 showing several QTLs for growth rate (GR) and backfat (BF).**

239

240 In this region we find 5 independent QTLs within this span of 15Mb, of which 3 within a 3Mb span. Within some
241 of the QTLs, we find SNPs with different and opposing effects. The majority of the top SNPs of the different QTLs
242 and effects are not in linkage disequilibrium (LD) (Table 2), indicating that these are mostly independently
243 segregating haplotypes.

244

245

246

247

248

249 Table 2: LD within the QTL rich 15MB region on chromosome 1 in Large White.

LD (R ²) / SNP	150364747	150364747	1	154978577	154978577	159788889	159788889	159821786	159821786	159869511	159869511	160883673	160883673	162020747	162020747	162062651	162062651	164838503	164838503	164909824	164909824
150364747		1		154978577																	
154978577	0.216699		1	159788889																	
159788889	0.207151		0.0420421		1	159821786															
159821786	0.0492199		0.00678435	0.280964		1	159869511														
159869511	0.104494	0.495845		0.0342459		0.00947161			1	160883673											
160883673	0.166053	0.696078		0.0550575		0.0154966	0.48608			1	162020747										
162020747	0.194158		0.0348452	0.726328		0.237485		0.0274089		0.0538396		1	162062651								
162062651	0.0639927		0.00931752	0.202506	0.677308		0.0112798		0.0187777		0.339906		1	164838503							
164838503	0.0195427		0.157152	0.0581801		0.00639335		0.0786844		0.219678		0.042347		0.00143272		1	164909824				
164909824	0.0425097		0.00175518	0.147268		0.00425724		0.000552646		0.00572898		0.131389		0.0052275		0.146082		1			

250 LD, Linkage Disequilibrium; Cell shading; orange: $R^2 = 0.40-0.60$, yellow: $R^2 = 0.60-0.70$, green: $R^2 > 0.70$

251

252 The QTLs at 150 and 154Mb in Large White both consist of only intergenic variants with allele frequencies
253 ranging from 30-35%. One of the positive effects we observe in the 3Mb span from 159-162Mb is due to a
254 missense SNP in the *MC4R* gene. This effect is represented by the top SNP at 160Mb in figure 5, which is in high
255 LD with the *MC4R* missense SNP. The SNP in the QTL at 160Mb for backfat, as well as the QTLs for both traits at
256 160Mb in Synthetic also show LD with the *MC4R* missense SNP.

257 The top SNP for growth rate in Large White for this whole region is located at 159,788,889bp with a MAF of 10%
258 and a negative effect on growth. This SNP and the variants that are in LD are all intergenic variants, located near
259 the *CDH20* (cadherin 20) gene. We also find significant intron variants of *CDH20*, however, some of these SNPs
260 have a frequency of 23% and a positive effect on growth, while others have a frequency of 3% and a negative
261 effect on growth. The top SNP of 23% MAF is located at 159,869,511bp and the top SNP of 3% MAF is located at
262 159,821,786bp. The same locus around the *CDH20* gene shows up in the Synthetic breed.

263 We looked at gene expression in this region in liver, muscle, spleen and lung. We found several SNPs between
264 159 and 161Mb to significantly affect the expression of the *PYGL* (glycogen phosphorylase L) gene, located at
265 180Mb on the same chromosome 1, an allosteric enzyme that catalyzes the rate-limiting step in glycogen
266 catabolism [17].

267

268

269

270 Discussion

271 In this study, we performed sequence based GWAS on a large scale with both an additive and non-additive
272 model, allowing us to identify novel and low frequent deleterious variants. By using a non-additive (recessive)
273 model, we identified completely novel QTLs compared to the additive model, which are in most cases extremely
274 significant due to their deleterious nature. As these recessive deleterious variants tend to be present with low
275 allele frequencies, it is essential to have large datasets when attempting to identify them through GWAS.
276 Especially when using WGS data, this leads to very computationally intense analyses. We experienced mainly
277 the high number of phenotypes to be a bottleneck for memory usage, as the genome can be split up in segments
278 to run parallel analysis. The computational limitations are naturally very dependent on the type of software used
279 and the available computing infrastructure. In our situation, we found a number of around 75,000 phenotypes
280 to be the maximum. This number is sufficient when mainly focusing on SNPs with MAFs above 1%, which was
281 the case in this study due to imputation accuracies. If in the future we would be able to accurately impute even
282 lower frequent SNPs with high accuracy, new methods would be needed to include a larger number of
283 phenotypes for GWAS.

284 We observed a total of 22 QTLs across the two traits and breeds, of which most will require further research to
285 proof the causal variants and the biological mechanism. However, for some of the QTLs we identified potential
286 causal variants causing a loss of function and therefore expected to impair gene function. We found some of
287 these variants to cause very poor performance and therefore proving very interesting candidates for selection.

288 One of these variants is located on chromosome 2, where we observed a QTL in the non-additive GWAS, leading
289 to a reduction in both growth rate and backfat. The most significant SNPs in this QTL are mainly intron variants
290 of *ADAMTS2*. We do not observe any deleterious variants in this gene specifically. Inactivation of *ADAMTS2* has
291 been associated with Ehlers-Danlos syndrome, a disorder affecting collagen formation and function [18].
292 Affected individuals suffer from hypermobile joints and flexible, fragile skin [19]. There are several mutations
293 known in several genes that can lead to development of this disorder. Though not a very common symptom,
294 short stature has been observed in some patients with Ehlers-Danlos syndrome [20]. The syndrome has been
295 observed in domestic animals including sheep and cattle, but not yet in pigs. Affected animals also display the
296 loose and fragile skin phenotype [21]. If the decreased growth we observe in pigs homozygous for this region

297 were to be caused by a similar syndrome, we would expect to observe similar phenotypes. This would require
298 further observation of homozygous animals. For now, since we do not observe deleterious variants in *ADAMTS2*
299 and are not aware of additional symptoms indicating Ehler-Danlos syndrome in these animals, we do not
300 consider this disorder to likely be the cause of the reduced growth. Another significant SNP in this QTL, though
301 not as significant as the top SNPs, is a missense SNP in *CDHR2* with a very strong deleterious effect. Previous
302 research has studied the function of *CDHR2* by knocking out the gene in mice. Knock-out animals showed a
303 decrease in body weight, likely due to absence of *CDHR2* leading to shorter microvilli and a lower packing density
304 in the intestine [14]. Based on these findings we expect this missense SNP could be the causal variant leading to
305 the observed decrease in growth and backfat.

306 Another recessive causal loss of function variant we managed to identify is located on chromosome 15, affecting
307 the *OBSL1* gene. This variant causes the strongest phenotypic effect we observed in all GWAS results.
308 Homozygous animals show a strong reduction in growth rate and increase in backfat thickness. We identified a
309 frameshift variant in *OBSL1* to be the causal mutation. Cytoskeletal adaptors play an important role in ensuring
310 structural integrity of cells by linking the internal cytoskeleton to the cells membrane [22]. Defects in *OBSL1* have
311 been found to lead to 3M-syndrome 2 in humans. Several cases have been studied and all mutations in *OBSL1*
312 causing the syndrome were null mutations within the first 6 exons of the gene, therefore affecting all transcripts
313 [23]. The variant we identified is located on exon 5 and causes a frameshift, therefore likely also leading to the
314 gene being fully defect. The most common symptom of 3M-syndrome is short stature due to growth restriction,
315 often accompanied by dysmorphic features and skeletal abnormalities [24]. Similar symptoms have been
316 observed in sheep with a defect in *OBSL1*, though unlike in humans, sheep homozygous for the defect are
317 stillborn [25]. 3M-syndrome has not yet been described in pigs before. We expect the identified frameshift
318 variant to cause a similar syndrome in pigs, explaining the severe reduction in growth we observe in homozygous
319 animals.

320 The *MPIG6B* gene, where we found a deleterious missense SNP in the Synthetic breed, hasn't been directly
321 associated with variations in growth/body size. However, this gene is essential for blood platelet production and
322 function. Previous research has shown that knock-out of the gene in mice leads to a reduced number of blood
323 platelets and the occurrence of enlarged platelets. Additionally, these animals showed increased production of
324 metalloproteinase, leading to increased shedding of cell-surface receptors [26].

325 We speculate that the missense SNP we identified might lead to similar issues in the blood of homozygous
326 animals, expressing overall lower performance including decreased growth.

327 Deleterious recessive variants are often observed segregating in a single breed [2]. Therefore, crossbred
328 offspring are generally not affected by these variants, which has been hypothesized to contribute to heterosis
329 [27]. We did identify one recessive stop-gain SNP present in both lines, in the *ANKRD55* gene. The presence of
330 this SNP can now be monitored and crossbred mating resulting in potential homozygous offspring can be
331 avoided.

332 We also found some interesting novel QTLs in our additive GWAS for which we have not yet managed to pin
333 down specific causal variants, but we identified genes that are likely involved. At the start of chromosome 2, we
334 found a highly significant QTL with a frequency of only 0.5%, leading to strongly increased backfat. In this QTL,
335 both the *INS* and *IGF2* genes are present. *IGF2* produces a protein important in growth regulation and is also
336 involved in glucose metabolism [28], and *INS* plays a role in carbohydrate and lipid metabolism by regulating
337 glucose uptake [29]. A QTL in *IGF2* has been previously identified to affect fat deposition in pigs [30]. Therefore,
338 we expect *IGF2* to most likely be the causal gene, but we have not yet found a specific variant linked to it. Finding
339 the causal variant is especially hard due to the extremely low frequency of the QTL.

340 One of the most difficult to analyze results is the small complex region on chromosome 1 with several significant
341 effects on growth rate and backfat. The regions with different effects overlapping with each other makes it very
342 challenging to identify causal variants for these QTLs. We did find several SNPs for both breeds that have a
343 significant effect on the expression of *PYGL*. *PYGL* functions to create an enzyme that breaks down glycogen into
344 glucose in the liver [31]. Glycogen levels influence fat metabolism [32], explaining how changes in expression of
345 this gene could lead to reduced or increased growth rate and backfat thickness. In Large White, the SNPs
346 affecting *PYGL* expression are associated with a positive effect on growth, whereas in Synthetic they are
347 associated with a negative effect on growth. This likely indicates that it's not the same causal variant affecting
348 *PYGL* expression in both breeds. Further in-depth investigation of this region will be needed to disentangle all
349 separate variants and effects in this QTL. This region highlights the benefit of using a high-resolution data set, as
350 previous analysis often considered this QTL to be caused only by the *MC4R* missense variant, while we can show
351 that several other variants and genes are involved.

352 In conclusion, by performing a large-scale sequence based GWAS using a non-additive model we identified
353 several rare, recessive, and deleterious variants with high impact on pig performance and production.
354 Additionally, the high-resolution capacity of this data set enabled us to detect multiple independent QTL effects
355 in the well-known *MC4R* region. These results provide a valuable resource for breeding and for further reduction
356 of the frequency of deleterious alleles.

357

358

359

360

361

362

363

364

365

366

367

368

369

370

371

372

373

374

375 Methods

376 Genotyping & Sequencing

377 All animals imputed to sequence were initially genotyped on either (Illumina) Geneseek custom 50K or 25K SNP
378 chips, with 50,689 SNPs and 26,894 SNPs respectively (Lincoln, NE, USA). The chromosomal positions were
379 determined based on the Sscrofa11.1 reference assembly [33]. SNPs located on autosomal chromosomes were
380 kept for further analysis. Next, the SNPs were filtered using the following requirements: Each marker had a MAF
381 greater than 0.01, and a call rate greater than 0.85, and each animal a call rate greater than 0.7. SNPs with a p-
382 value below 1E-5 for the Hardy-Weinberg equilibrium exact test were also discarded. All pre-processing steps
383 were performed using Plink v1.90b3.30 [34]. The reference population for imputation to 660K was genotyped
384 on the Axiom porcine 660K SNP array from Affymetrix. Quality control was as described above for the 50K
385 genotyping.

386 DNA sequencing of the reference population was performed on the Illumina Hiseq. The reads were aligned to
387 Sus Scrofa 11.1 [33] using BWA-MEM v0.7.17 [35]. Variant calling was performed with Freebayes v1.3.1 with
388 settings --min-base-quality 20, --min-mapping-quality 30, --min-alternate-fraction 0.2, --haplotype-length 0 and
389 --min-alternate-count 3 [36]. Variants with a quality score below 20 were discarded. Variants were annotated
390 using the Ensembl variant effect predictor (VEP, release 103) [11].

391 Imputation

392 For imputation from 50K to 660K density we used Fimpute v3.0 [37]. The reference population consisted of 3500
393 animals of different breeds.

394 The first step in imputing to sequence is phasing of the haplotypes. For the phasing we used Beagle 5.4, with a
395 window of 20, overlap of 5, Ne of 100 and 16 threads [38]. We then ran the conform-gt tool to get consistent
396 allele coding between the reference and target VCF files. For the actual imputation we used Beagle 5.4, with a
397 window of 3, Ne of 100 and 20 threads [4]. For Large White, one round of imputation to sequence was performed
398 for 40,000 animals, and another round for 80,000 animals. We then merged the resulting VCF files of both
399 imputation runs into one file for each chromosome using bcftools merge [39], giving us sequence data on a total
400 of 117,244 animals after some were lost in the phasing steps.

401 For Synthetic we performed imputation to sequence on 80,000 animals. We used Plink v1.90b3.38 [34] to recode
402 the VCF files so that all major alleles were set as reference alleles. To obtain more information on each SNP we
403 used the bcftools fill-tags plugin [39]. The reference population consisted of 884 whole genome sequences for
404 the imputation of the first 40,000 Large White animals, and 1069 whole genome sequences for the second
405 imputation of 80,000 animals as well as the Synthetic animals. This reference population contained animals of
406 the Large White, Synthetic, Landrace, Duroc and Pietrain breeds.

407 **Genome-Wide Association Studies (GWAS)**

408 We performed single-SNP GWAS on the imputed sequence data using GCTA v1.93.2 [40] with the following linear
409 model:

410 $y_{*k} = \mu + X\beta + u_k + e_k$

411 where y_{*k} is the pre-corrected phenotype of the k animal (pre-corrected for all non-genetic effects); μ is the
412 average of the pre-corrected phenotype; X is the genotype, coded as 0, 1, or 2 copies of one of the alleles of the
413 k animal for the evaluated SNP; β is the unknown allele substitution effect of the evaluated SNP; u_k is the
414 residual polygenic effect, assuming $u \sim N(\mathbf{0}, \mathbf{G} \sigma_{2u}^2)$, which accounted for the (co)variances between animals
415 due to relationships by formation of a \mathbf{G} matrix (genomic numerator relationship matrix build using the imputed
416 genotypes), σ_{2u}^2 is the additive genetic variance; and e_k is the random residual effect which was assumed to be
417 distributed as $\sim N(\mathbf{0}, \mathbf{I} \sigma_{2e}^2)$.

418 To run the non-additive model GWAS, all heterozygote genotypes were set to 0/0 to test the phenotypes of
419 wildtype and heterozygous animals against homozygous animals.

420 **Gene expression**

421 We had access to a gene expression dataset including expression data from 100 crossbred animals in four tissues:
422 liver, spleen, lung and muscle [41].

423

424

425

426 **Phenotypes**

427 The phenotypes were pre-corrected for non-genetic effects. For the Large white breed we used 67,280 growth
428 rate phenotypes and 72,061 phenotypes for backfat thickness. For the Synthetic breed we used 74,145
429 phenotypes for both traits.

430 **Validation of causal 5 bp *OBSL1* Deletion**

431 PCR was done using 60 ng of genomic DNA, with 0.4 μ m of each primer, 1.8 mM MgCl₂, and 25 units/ml OneTaq®
432 DNA Polymerase (OneTaq® 2X Master Mix with Standard Buffer, New England Biolabs) in manufacturer's PCR
433 buffer in a final volume of 12 μ l. Initial denaturation for 1 min at 95°C was followed by 35 cycles of 95°C for 30
434 s, 55°C for 45 s, 72°C 90 s, followed by a 5 min extension 72°C. PCR primers for *OBSL1* are
435 ACGTCCTTGATCCTGTCTGC forward and CTCTCCACCATCATCCAGGG reverse. The forward primer was dye-
436 labeled with either 6-FAM to produce a fluorescently labeled PCR product detectable on ABI 3730 DNA
437 sequencer (Applied Biosystems). Fragment sizes were determined using GeneMapper software 5 from ABI.

438 **Further analysis & figures**

439 To perform linkage disequilibrium (LD) analysis we used Plink v1.90b3.38 with settings --ld-window-r2 0 --ld-
440 window 9999999 --ld-window-kb 100000 [34]. To assess how deleterious a variant is we considered the SIFT
441 score as given by the VEP [11], as well as the Combined Annotation Dependent Depletion (CADD) score [42],
442 adapted for pigs (pCADD, [13]). Boxplots, heatmaps and manhattanplots were made using the python packages
443 seaborn [43], heatmapz [44] and QMplot [45] respectively. Additionally, pandas [46] and matplotlib [47] were
444 used in creating the figures.

445
446
447
448
449
450
451

452 Acknowledgements

453 We thank Imke Leemans and Frank van Haaren for their help in farm communication and data collection.

454

455

456

457

458

459

460

461

462

463

464

465

466

467

468

469

470

471

472

473

474

475

476

477

478

479

480

481 References

482 1. Meuwissen TH, Hayes BJ, Goddard ME. Prediction of total genetic value using genome-wide dense
483 marker maps. *Genetics*. 2001;157: 1819–1829. doi:10.1093/genetics/157.4.1819

484 2. Bosse M, Megens H-J, Derkx MFL, Cara ÁMR de, Groenen MAM. deleterious alleles in the context of
485 domestication, inbreeding, and selection. *Evol Appl*. 2019;12: 6. doi:10.1111/eva.12691

486 3. Sariya S, Lee JH, Mayeux R, Vardarajan BN, Reyes-Dumeyer D, Manly JJ, et al. Rare Variants Imputation in
487 Admixed Populations: Comparison Across Reference Panels and Bioinformatics Tools. *Front Genet*.
488 2019;10. Available: <https://www.frontiersin.org/articles/10.3389/fgene.2019.00239>

489 4. Browning BL, Zhou Y, Browning SR. A One-Penny Imputed Genome from Next-Generation Reference
490 Panels. *Am J Hum Genet*. 2018;103: 338–348. doi:10.1016/j.ajhg.2018.07.015

491 5. Qanbari S. On the Extent of Linkage Disequilibrium in the Genome of Farm Animals. *Front Genet*.
492 2020;10. Available: <https://www.frontiersin.org/articles/10.3389/fgene.2019.01304>

493 6. Xue Y, Liu S, Li W, Mao R, Zhuo Y, Xing W, et al. Genome-Wide Association Study Reveals Additive and
494 Non-Additive Effects on Growth Traits in Duroc Pigs. *Genes*. 2022;13: 1454. doi:10.3390/genes13081454

495 7. Matika O, Robledo D, Pong-Wong R, Bishop SC, Riggio V, Finlayson H, et al. Balancing selection at a
496 premature stop mutation in the myostatin gene underlies a recessive leg weakness syndrome in pigs.
497 *PLoS Genet*. 2019;15: e1007759. doi:10.1371/journal.pgen.1007759

498 8. Derkx MFL, Gjuvsland AB, Bosse M, Lopes MS, van Son M, Harlizius B, et al. Loss of function mutations in
499 essential genes cause embryonic lethality in pigs. *PLoS Genet*. 2019;15: e1008055.
500 doi:10.1371/journal.pgen.1008055

501 9. Liu H-M, Zheng J-P, Yang D, Liu Z-F, Li Z, Hu Z-Z, et al. Recessive/dominant model: Alternative choice in
502 case-control-based genome-wide association studies. *PLOS ONE*. 2021;16: e0254947.
503 doi:10.1371/journal.pone.0254947

504 10. Reynolds EGM, Neeley C, Lopdell TJ, Keehan M, Dittmer K, Harland CS, et al. Non-additive association
505 analysis using proxy phenotypes identifies novel cattle syndromes. *Nat Genet.* 2021;53: 949–954.
506 doi:10.1038/s41588-021-00872-5

507 11. McLaren W, Gil L, Hunt SE, Riat HS, Ritchie GRS, Thormann A, et al. The Ensembl Variant Effect Predictor.
508 *Genome Biol.* 2016;17: 122. doi:10.1186/s13059-016-0974-4

509 12. Sim N-L, Kumar P, Hu J, Henikoff S, Schneider G, Ng PC. SIFT web server: predicting effects of amino acid
510 substitutions on proteins. *Nucleic Acids Res.* 2012;40: W452–W457. doi:10.1093/nar/gks539

511 13. Groß C, Derkx M, Megens H-J, Bosse M, Groenen MAM, Reinders M, et al. pCADD: SNV prioritisation in
512 *Sus scrofa*. *Genet Sel Evol.* 2020;52: 4. doi:10.1186/s12711-020-0528-9

513 14. Pinette JA, Mao S, Millis BA, Krystofiak ES, Faust JJ, Tyska MJ. Brush border protocadherin CDHR2
514 promotes the elongation and maximized packing of microvilli in vivo. *Mol Biol Cell.* 2019;30: 108–118.
515 doi:10.1091/mbc.E18-09-0558

516 15. Martin FJ, Amode MR, Aneja A, Austine-Orimoloye O, Azov AG, Barnes I, et al. Ensembl 2023. *Nucleic
517 Acids Res.* 2023;51: D933–D941. doi:10.1093/nar/gkac958

518 16. Oliveira HC, Derkx MFL, Lopes MS, Madsen O, Harlizius B, van Son M, et al. Fine Mapping of a Major
519 Backfat QTL Reveals a Causal Regulatory Variant Affecting the CCND2 Gene. *Front Genet.* 2022;13:
520 871516. doi:10.3389/fgene.2022.871516

521 17. Dall’Olio S, Schiavo G, Gallo M, Bovo S, Bertolini F, Buttazzoni L, et al. Candidate gene markers associated
522 with production, carcass and meat quality traits in Italian Large White pigs identified using a selective
523 genotyping approach. *Livest Sci.* 2020;240: 104145. doi:10.1016/j.livsci.2020.104145

524 18. Colige A, Nuytinck L, Hausser I, van Essen AJ, Thiry M, Herens C, et al. Novel types of mutation
525 responsible for the dermatosparactic type of Ehlers-Danlos syndrome (Type VIIC) and common
526 polymorphisms in the ADAMTS2 gene. *J Invest Dermatol.* 2004;123: 656–663. doi:10.1111/j.0022-
527 202X.2004.23406.x

528 19. Miklovic T, Sieg VC. Ehlers-Danlos Syndrome. StatPearls. Treasure Island (FL): StatPearls Publishing;
529 2023. Available: <http://www.ncbi.nlm.nih.gov/books/NBK549814/>

530 20. Ishiguro H, Yagasaki H, Horiuchi Y. Ehlers-Danlos Syndrome in the Field of Psychiatry: A Review. *Front*
531 *Psychiatry*. 2022;12. Available: <https://www.frontiersin.org/articles/10.3389/fpsyg.2021.803898>

532 21. Ehler-Danlos Syndrome (Cutaneous asthenia, dermatosparaxis). In: *Veterinary Practice* [Internet]. 1 Oct
533 2016 [cited 27 Jul 2023]. Available: <https://www.veterinary-practice.com/article/ehler-danlos->
534 [syndrome-cutaneous-asthenia-dermatosparaxis](#)

535 22. Geisler SB, Robinson D, Hauringa M, Raeker MO, Borisov AB, Westfall MV, et al. Obscurin-Like 1, ODSL1,
536 is a novel cytoskeletal protein related to obscurin. *Genomics*. 2007;89: 521–531.
537 doi:10.1016/j.ygeno.2006.12.004

538 23. Hanson D, Murray PG, Sud A, Temtamy SA, Aglan M, Superti-Furga A, et al. The Primordial Growth
539 Disorder 3-M Syndrome Connects Ubiquitination to the Cytoskeletal Adaptor ODSL1. *Am J Hum Genet*.
540 2009;84: 801–806. doi:10.1016/j.ajhg.2009.04.021

541 24. Keskin M, Muratoğlu Şahin N, Kurnaz E, Bayramoğlu E, Savaş Erdeve Ş, Aycan Z, et al. A Rare Cause of
542 Short Stature: 3M Syndrome in a Patient with Novel Mutation in ODSL1 Gene. *J Clin Res Pediatr*
543 *Endocrinol*. 2017;9: 91–94. doi:10.4274/jcrpe.3238

544 25. Woolley SA, Hayes SE, Shariflou MR, Nicholas FW, Willet CE, O'Rourke BA, et al. Molecular basis of a new
545 ovine model for human 3M syndrome-2. *BMC Genet*. 2020;21: 106. doi:10.1186/s12863-020-00913-8

546 26. Mazharian A, Wang Y-J, Mori J, Bem D, Finney B, Heising S, et al. Mice Lacking the ITIM-Containing
547 Receptor G6b-B Exhibit Macrothrombocytopenia and Aberrant Platelet Function. *Sci Signal*. 2012;5:
548 ra78–ra78. doi:10.1126/scisignal.2002936

549 27. Li L, Lu K, Chen Z, Mu T, Hu Z, Li X. Dominance, Overdominance and Epistasis Condition the Heterosis in
550 Two Heterotic Rice Hybrids. *Genetics*. 2008;180: 1725–1742. doi:10.1534/genetics.108.091942

551 28. Sélénou C, Brioude F, Giabicani E, Sobrier M-L, Netchine I. IGF2: Development, Genetic and Epigenetic
552 Abnormalities. *Cells*. 2022;11. doi:10.3390/cells11121886

553 29. INS insulin [Homo sapiens (human)] - Gene - NCBI. [cited 7 Sep 2023]. Available:
554 <https://www.ncbi.nlm.nih.gov/gene/3630>

555 30. Nezer C, Moreau L, Brouwers B, Coppieters W, Detilleux J, Hanset R, et al. An imprinted QTL with major
556 effect on muscle mass and fat deposition maps to the IGF2 locus in pigs. *Nat Genet*. 1999;21: 155–156.
557 doi:10.1038/5935

558 31. PYGL gene: MedlinePlus Genetics. [cited 11 Aug 2023]. Available:
559 <https://medlineplus.gov/genetics/gene/pygl/>

560 32. Flatt JP. Glycogen levels and obesity. *Int J Obes Relat Metab Disord J Int Assoc Study Obes*. 1996;20
561 Suppl 2: S1-11.

562 33. Warr A, Affara N, Aken B, Beiki H, Bickhart DM, Billis K, et al. An improved pig reference genome
563 sequence to enable pig genetics and genomics research. *GigaScience*. 2020;9: giaa051.
564 doi:10.1093/gigascience/giaa051

565 34. Chang CC, Chow CC, Tellier LC, Vattikuti S, Purcell SM, Lee JJ. Second-generation PLINK: rising to the
566 challenge of larger and richer datasets. *GigaScience*. 2015;4: 7. doi:10.1186/s13742-015-0047-8

567 35. Li H. Aligning sequence reads, clone sequences and assembly contigs with BWA-MEM. *arXiv*; 2013.
568 doi:10.48550/arXiv.1303.3997

569 36. Garrison E, Marth G. Haplotype-based variant detection from short-read sequencing. *arXiv*; 2012.
570 doi:10.48550/arXiv.1207.3907

571 37. Sargolzaei M, Chesnais JP, Schenkel FS. A new approach for efficient genotype imputation using
572 information from relatives. *BMC Genomics*. 2014;15: 478. doi:10.1186/1471-2164-15-478

573 38. Browning BL, Tian X, Zhou Y, Browning SR. Fast two-stage phasing of large-scale sequence data. *Am J
574 Hum Genet*. 2021;108: 1880–1890. doi:10.1016/j.ajhg.2021.08.005

575 39. Li H. A statistical framework for SNP calling, mutation discovery, association mapping and population
576 genetical parameter estimation from sequencing data. *Bioinformatics*. 2011;27: 2987–2993.
577 doi:10.1093/bioinformatics/btr509

578 40. Yang J, Lee SH, Goddard ME, Visscher PM. GCTA: A Tool for Genome-wide Complex Trait Analysis. *Am J
579 Hum Genet.* 2011;88: 76–82. doi:10.1016/j.ajhg.2010.11.011

580 41. Gòdia M, Derkx M f. I., Harlizius B, Madsen O, Groenen M a. m. 558. Unravelling regulatory variants
581 affecting gene expression in four porcine tissues. *Proceedings of 12th World Congress on Genetics
582 Applied to Livestock Production (WCGALP)*. Wageningen Academic Publishers; 2022. pp. 2313–2316.
583 doi:10.3920/978-90-8686-940-4_558

584 42. Rentzsch P, Witten D, Cooper GM, Shendure J, Kircher M. CADD: predicting the deleteriousness of
585 variants throughout the human genome. *Nucleic Acids Res.* 2019;47: D886–D894.
586 doi:10.1093/nar/gky1016

587 43. Waskom M, Gelbart M, Botvinnik O, Ostblom J, Hobson P, Lukauskas S, et al. mwaskom/seaborn: v0.12.2
588 (December 2022). Zenodo; 2022. doi:10.5281/zenodo.7495530

589 44. dylan-profiler/heatmaps. dylan-profiler; 2023. Available: <https://github.com/dylan-profiler/heatmaps>

590 45. Huang S. QMplot: A Python tool for creating high-quality manhattan and Q-Q plots from GWAS results.
591 2023. Available: <https://github.com/ShujiaHuang/qmplot>

592 46. McKinney W. Data Structures for Statistical Computing in Python. Austin, Texas; 2010. pp. 56–61.
593 doi:10.25080/Majora-92bf1922-00a

594 47. Team TMD. Matplotlib: Visualization with Python. Zenodo; 2023. doi:10.5281/zenodo.8236669

595

596

597 Supporting information

598 **S1 Figure: Overview of the imputation and GWAS pipeline.**

599 **S2 Table: Top SNPs for all QTLs resulting from the GWAS.**

600 **S3 Table: Validation of causal 5bp *OBSL1* deletion.**